

Quasiparticle relaxation in optically excited high-Q superconducting resonators

R. Barends,¹ J. J. A. Baselmans,² S. J. C. Yates,² J. R. Gao,^{1,2} J. N. Hovenier,¹ and T. M. Klapwijk¹

¹*Kavli Institute of NanoScience, Faculty of Applied Sciences,
Delft University of Technology, Lorentzweg 1, 2628 CJ Delft, The Netherlands*

²*SRON Netherlands Institute for Space Research,
Sorbonnelaan 2, 3584 CA Utrecht, The Netherlands*

(Dated: June 5, 2008)

The quasiparticle relaxation time in superconducting films has been measured as a function of temperature using the response of the complex conductivity to photon flux. For tantalum and aluminium, chosen for their difference in electron-phonon coupling strength, we find that at high temperatures the relaxation time increases with decreasing temperature, as expected for electron-phonon interaction. At low temperatures we find in both superconducting materials a saturation of the relaxation time, suggesting the presence of a second relaxation channel not due to electron-phonon interaction.

PACS numbers: 74.25.Nf, 74.40.+k

The equilibrium state of a superconductor at finite temperatures consists of the Cooper pair condensate and thermally excited quasiparticles. The quasiparticle density n_{qp} decreases exponentially with decreasing temperature. These charge carriers control the high frequency (ω) response of the superconductor through the complex conductivity $\sigma_1 - i\sigma_2$. At nonzero frequencies the real part σ_1 denotes the conductivity by quasiparticles and the imaginary part σ_2 is due to the superconducting condensate [1, 2]. When the superconductor is driven out of equilibrium it relaxes back to the equilibrium state by the redistribution of quasiparticles over energy and by recombination of quasiparticles to Cooper pairs. The recombination is a binary reaction, quasiparticles with opposite wavevector and spin combine, and the remaining energy is transferred to another excitation. The latter process is usually controlled by the material dependent electron-phonon interaction [3, 4]. With decreasing temperatures the recombination time increases exponentially reflecting the reduced availability of quasiparticles. Here, we report relaxation time measurements in superconducting films far below the critical temperature T_c . We find strong deviations from exponentially rising behavior, which we attribute to the emergence of an additional relaxation channel in the superconducting films.

We have measured the time dependence of the complex conductivity of superconducting films after applying an optical photon pulse. In addition, the noise spectrum is measured in the presence of a continuous photon flux [5]. The superconducting film is patterned as a planar microwave resonator. The resonator is formed by a meandering coplanar waveguide (CPW), with the central line $3 \mu\text{m}$ and the slits $2 \mu\text{m}$ wide, and is coupled to a feedline, see Fig. 1a [6]. The complex conductivity results in a kinetic inductance $L_k \propto 1/d\omega\sigma_2$, for thin films with thickness d , which is due to the inertia of the Cooper pair condensate. It sets together with the length of the central line the resonance frequency: $\omega_0 = 2\pi/4l\sqrt{(L_g + L_k)C}$,

with l the length of a quarterwave resonator, L_g the geometric inductance and C the capacitance, both per unit length. The variation in kinetic inductance due to photons is connected to the quasiparticle density n_{qp} by $\delta L_k/L_k = \frac{1}{2}\delta n_{qp}/n_{cp}$, with n_{cp} the Cooper pair density

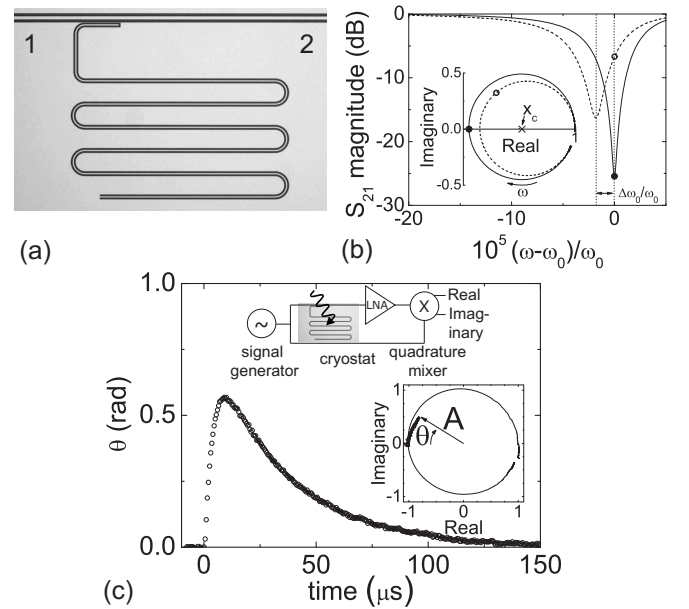


FIG. 1: (a) A quarter wavelength resonator, capacitively coupled to a feedline, formed by the superconducting film (gray) interrupted by slits (black). (b) The resonator exhibits a dip in the magnitude and circle in the complex plane (inset) of the feedline transmission S_{21} . (c) The feedline transmission is converted into a phase θ and amplitude A using the equilibrium resonance circle as reference (right inset). The response to an optical pulse of length $0.5 \mu\text{s}$ (at $t=0$) (open circles) exhibits an initial rise due to the response time ($3.7 \mu\text{s}$) of the resonator and subsequently follows an exponential decay ($34 \mu\text{s}$) (dashed), reflecting the restoration of equilibrium (Eq. 1). The response is measured with a signal generator, low noise amplifier (LNA) and quadrature mixer (upper inset).

($n_{qp} \ll n_{cp}$). Resonance frequencies used lie between 3-6 GHz. For a quarterwave resonator at 6 GHz, the length of the meandering superconducting CPW-line is 5 mm. The resonator is capacitively coupled by placing a part parallel to the feedline.

The resonators are made from superconducting materials with different electron-phonon interaction strengths, tantalum (strong interaction) and aluminium (weak interaction). The tantalum film, 150 nm thick, is sputtered on a high resistivity silicon substrate. A 6 nm thick niobium seed layer is used to promote the growth of the desired tantalum alpha phase [7]. The critical temperature T_c is 4.43 K, the low temperature resistivity ρ is $8.4 \mu\Omega\text{cm}$ and the residual resistance ratio (RRR) is 3.0. A 100 nm thick aluminium film is sputtered on silicon ($T_c=1.25$, $\rho=1.3 \mu\Omega\text{cm}$, $RRR=3.7$). Alternatively, a film of 250 nm thick is sputtered on silicon ($T_c=1.22$, $\rho=1.0 \mu\Omega\text{cm}$, $RRR=6.9$) and another one of 250 nm is sputtered on A-plane sapphire ($T_c=1.20$, $\rho=0.25 \mu\Omega\text{cm}$, $RRR=11$). The samples are patterned using optical lithography, followed by wet etching for aluminium and reactive ion etching for tantalum. For both materials quality factors in the order of 10^6 are reached. The sample is cooled in a cryostat with an adiabatic demagnetization refrigerator. The sample space is surrounded by a cryoperm and a superconducting magnetic shield. Alternatively, the sample is cooled in a cryostat with a ^3He sorption cooler without magnetic shields. A GaAsP LED (1.9 eV) acts as photon source, fibre-optically coupled to the sample box.

The complex transmission S_{21} of the circuit is measured by sweeping the frequency of the signal applied along the feedline (Fig. 1a). Near the resonance frequency ω_0 the feedline transmission exhibits a decrease in magnitude and traces a circle in the complex plane (full lines in Fig. 1b). A non-equilibrium state results in a resonance frequency shift and broadening of the dip, and a reduction and shift of the resonance circle in the complex plane (dashed lines in Fig. 1b). The actual signals (filled dot and open circle in Fig. 1b) are obtained by sending a continuous wave at the equilibrium resonance frequency ω_0 through the feedline, which is amplified and mixed with a copy of the original signal in a quadrature mixer, whose output gives the real and imaginary part of the feedline transmission (upper inset Fig. 1c). The non-equilibrium response (open circle), compared to the equilibrium response (filled dot), is characterized by a changed phase θ and amplitude A , referred to a shifted origin in the complex plane (from the equilibrium position x_c).

The phase θ with respect to the resonance circle center x_c is given by $\theta = \arctan[\text{Im}(S_{21})/(x_c - \text{Re}(S_{21}))]$ and is related to the change in resonance frequency by: $\theta = -4Q \frac{\delta\omega_0}{\omega_0}$, with Q the resonator loaded quality factor [6]. A related change in L_k is given by $\delta\omega_0/\omega_0 = -\frac{\alpha}{2} \delta L_k/L_k$, with α the ratio of the kinetic to the total inductance. The phase θ is therefore a direct measure of the change

in complex conductivity (given in the dirty limit by):

$$\theta = -2\alpha Q \frac{\delta\sigma_2}{\sigma_2} \left(f(E), \Delta \right), \quad (1)$$

with $f(E)$ the electronic distribution function characterizing the non-equilibrium and Δ the superconductor energy gap.

The amplitude A depends predominantly on σ_1 and to a smaller degree on σ_2 . The amplitude is determined by the complex transmission S_{21} by: $A = \sqrt{[\text{Re}(S_{21}) - x_c]^2 + \text{Im}(S_{21})^2} / (1 - x_c)$. On resonance $S_{21} = Q_c / (Q_c + Q_u)$ with $Q_u \propto \sigma_2 / \sigma_1$ the unloaded resonator quality factor and Q_c the coupling quality factor, leading to

$$A = 1 - 2 \frac{Q}{Q_u} \left[\frac{\delta\sigma_1}{\sigma_1} \left(f(E), \Delta \right) - \frac{\delta\sigma_2}{\sigma_2} \left(f(E), \Delta \right) \right]. \quad (2)$$

By measuring A and θ in the frequency- and time-domain we obtain direct information on the relaxation through the complex conductivity of the superconducting films.

A typical pulse response is shown in Fig. 1c. The initial rise of the phase θ is due to the response time of the resonator. The relaxation shows up as an exponential decay. The right inset of Fig. 1c shows the evolution of the response in the transformed polar plane. These data are interpreted as governed by one relaxation time. This is justified by performing measurements of the noise spectrum and applying the analysis by Wilson *et al.* [5]. Since the superconducting condensate and the quasiparticle excitations form a two-level system a Lorentzian spectrum is expected, with the relaxation time determining the roll-off frequency. If more dominant relaxation processes are present, the noise spectrum is no longer a single Lorentzian [8]. We have studied the superconducting films under exposure to a *continuous* photon flux. Our films are exposed to an optical white noise signal due to photon shot noise, resulting in fluctuations in $f(E)$. Where a single time τ determines the relaxation process the phase or amplitude noise spectrum is

$$S_{\theta,A} = \frac{2\hbar\Omega}{P} \frac{r_{\theta,A}}{1 + (2\pi f\tau)^2}, \quad (3)$$

with P the absorbed power, $\hbar\Omega$ the photon energy, and $r_{\theta,A}$ denoting the responsivity of the phase or amplitude to an optical signal.

The measured noise power spectra of the amplitude and phase of a tantalum sample are shown in Fig. 2. In equilibrium the amplitude noise spectrum (dashed blue line) is flat over the full range, and the phase noise (solid blue line) follows $1/f^a$ with $a \approx 0.25$. The amplitude noise is due to the amplifier, remaining unchanged at frequencies far away from ω_0 while the phase noise is dominated by resonator noise [9, 10], rolling off at a frequency corresponding to the resonator response time (0.5 μs). Under a continuous photon flux we observe excess noise

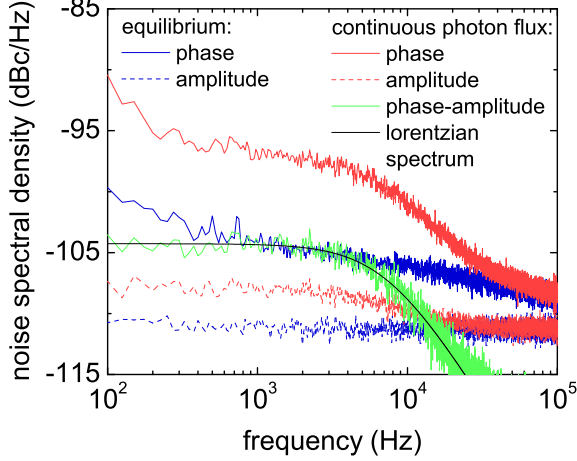


FIG. 2: (Color online) The power spectral density of phase (solid line) and amplitude (dashed) in equilibrium (blue) and under a continuous photon flux (red) at a bath temperature of 310 mK. The cross-power spectral density (solid green) under a continuous photon flux follows a single pole Lorentzian spectrum, $S \propto [1 + (2\pi f\tau)^2]^{-1}$, with a characteristic time of $21.7 \pm 0.3 \mu\text{s}$ (solid black). The response time of the resonator is $0.5 \mu\text{s}$.

in both amplitude (dashed red line) and phase (solid red line) that rolls off to the equilibrium value around 8 kHz.

The difference in noise levels is equal to the difference in responsivity: $r_A/r_\theta = 0.23$ (-13 dB), measured for this sample. In addition, we estimate, based on 20 pW optical power absorbed by the resonator, a phase noise level of -94 dBc/Hz due to photon shot noise, which is close to the observed value. Thus we conclude that the excess noise is due to variations in $f(E)$ induced by the photon flux. In order to eliminate the system and resonator noise we calculate the phase-amplitude cross-power spectral density (solid green line). We find that its spectrum is real, indicating that variations in $f(E)$ appear as fluctuations in the amplitude and phase without relative time delay, and that the data follow a Lorentzian spectrum with a single time. The time measured in the pulse response ($23.0 \pm 0.5 \mu\text{s}$) agrees with the one determined from the noise spectrum ($21.7 \pm 0.3 \mu\text{s}$). We have checked at several bath temperatures and found, also for aluminium samples, only a single time. We conclude that the relaxation time is the single dominant time in the recovery of equilibrium.

The measured relaxation times for temperatures down to 50 mK are displayed in Fig. 3. The data shown are representative for the relaxation times found in all samples of different films. In the high temperature regime ($T/T_c \gtrsim 0.175$) the relaxation times increase for decreasing bath temperature in a similar manner for both tantalum and aluminium samples until a new regime is en-

tered around $T/T_c \sim 0.15$. The tantalum samples clearly show a non-monotonic temperature dependence, exhibiting a maximum near $T/T_c \sim 0.15$. Two aluminium films show a less pronounced non-monotonic temperature dependence. We do not see a non-monotonic temperature dependence in samples of aluminium with the lowest level of disorder (highest RRR). Below $T/T_c \sim 0.1$ the relaxation times become temperature independent at a plateau value of $25\text{--}35 \mu\text{s}$ for Ta, $390 \mu\text{s}$ for 100 nm thick Al on Si, $600 \mu\text{s}$ for 250 nm thick Al on Si and $860 \mu\text{s}$ for 250 nm thick Al on sapphire.

The relaxation times for aluminium are measured in half wavelength resonators where the central line is isolated from the ground plane. For the directly connected quarter wavelength resonators a length dependence was found. For tantalum the values are found to be length independent in both cases. Consequently, the data shown are not influenced by quasiparticle outdiffusion. Also, the relaxation times remain unchanged when instead of an optical pulse a microwave pulse at frequency ω_0 is used. In this method only quasiparticle excitations near the gap energy are created by the pair-breaking current. This observation leads us to believe that the observed decay is due to recombination of quasiparticles with energies near the gap.

The exponential temperature dependence for $T/T_c \gtrsim 0.175$ is consistent with the theory of recombination by electron-phonon interaction [4]. The dotted lines in Fig. 3 follow the expression for the recombination time,

$$\frac{1}{\tau_{rec}} = \frac{1}{\tau_0} \sqrt{\pi} \left(\frac{2\Delta}{kT_c} \right)^{5/2} \sqrt{\frac{T}{T_c}} e^{-\frac{\Delta}{kT}}, \quad (4)$$

with τ_0 a material-specific electron-phonon scattering time. We find for 150 nm Ta on Si $\tau_0 = 42 \pm 2 \text{ ns}$

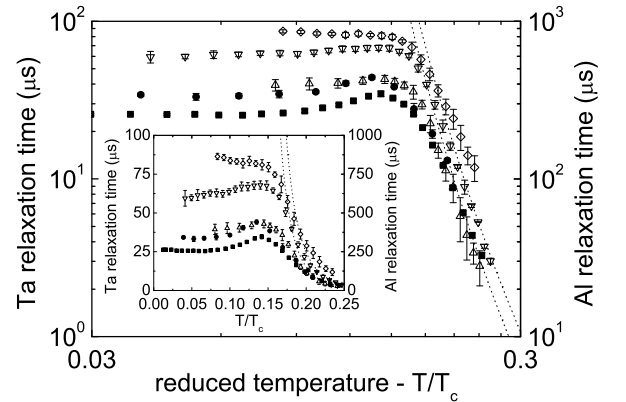


FIG. 3: The relaxation times as a function of reduced bath temperature for 150 nm Ta on Si (■, ●), 100 nm Al on Si (△), 250 nm Al on Si (▽) and 250 nm Al on sapphire (◇) samples. The inset shows the same data on a linear scale. The dotted lines are fits to the data using Eq. 4.

and for 250 nm Al on Si $\tau_0 = 687 \pm 6$ ns. The deviation from the exponential rise and the low temperature behavior is incompatible with the established theory for electron-phonon relaxation. We assume that an additional relaxation channel [11] is dominant at low temperatures, where the electron-phonon mechanism becomes too slow.

In previous experiments using superconducting tunnel junctions a similar saturation in the quasiparticle loss has been reported. For photon detectors inverse loss rates in the order of tens of microseconds have been found for tantalum [12, 13, 14, 15] and hundreds of microseconds for aluminium [6]. Some of these experiments also indicated a non-monotonic temperature dependence [16]. Most of these observations have been attributed to trapping states at surfaces or in dielectrics. The fact that our similar experimental results occur in simple superconducting films and two different materials suggests that processes in the superconducting film itself lead to the observed low temperature behavior.

The observed saturation in the relaxation times in our samples is reminiscent of experiments in normal metals on inelastic scattering in non-thermal distributions and on dephasing in weak localization studies. The apparent saturation of the dephasing time and the strong quasiparticle energy exchange at low temperatures have been shown to be caused by dilute concentrations of magnetic impurities [17, 18, 19, 20]. It is known that in superconductors a large density of magnetic impurities decreases the critical temperature. For dilute magnetic impurities the local properties are most important. In experiments with magnetic adatoms impurity bound excitations arise [21], tails in the density of states within the gap might form and the formation of an intragap band with growing impurity concentration are predicted [22, 23]. In ongoing experiments we observe a gradual decrease of the relaxation time with an increasing ion-implanted magnetic impurity concentration (0-100 ppm). However, disorder plays a role as well and further experiments are needed to clarify possible relaxation processes [24].

In conclusion, we find that the quasiparticle relaxation times, probed by means of the complex conductivity, saturate for both tantalum and aluminium, below a tenth of the critical temperature. We suggest that the saturation of the relaxation time is due to the presence of a relaxation channel, which is not caused by the conventional process dominated by electron-phonon interaction.

The authors thank Y. J. Y. Lankwarden for fabrication of the devices, A. G. Kozorezov, A. A. Golubov and R. A. Hijmering for helpful discussions and H. F. C. Hoovers for support. The work was supported by RadioNet (EU) under contract no. RII3-CT-2003-505818 and the

Netherlands Organisation for Scientific Research (NWO).

-
- [1] M. Tinkham, *Introduction to Superconductivity* (McGraw-Hill, New York, 1996).
 - [2] D. C. Mattis and J. Bardeen, Phys. Rev. **111**, 412 (1958).
 - [3] B. I. Miller and A. H. Dayem, Phys. Rev. Lett. **18**, 1000 (1967).
 - [4] S. B. Kaplan, C. C. Chi, D. N. Langenberg, J. J. Chang, S. Jafarey, and D. J. Scalapino, Phys. Rev. B **14**, 4854 (1976).
 - [5] C. M. Wilson, L. Frunzio, and D. E. Prober, Phys. Rev. Lett. **87**, 067004 (2001).
 - [6] P. K. Day, H. G. LeDuc, B. A. Mazin, A. Vayonakis, and J. Zmuidzinas, Nature **425**, 817 (2003).
 - [7] D. W. Face and D. E. Prober, J. Vac. Sci. Tech. A **5**, 3408 (1987).
 - [8] C. M. Wilson and D. E. Prober, Phys. Rev. B **69**, 094524 (2004).
 - [9] J. Gao, J. Zmuidzinas, B. A. Mazin, H. G. LeDuc, and P. K. Day, Appl. Phys. Lett. **90**, 102507 (2007).
 - [10] R. Barends, H. L. Hortensius, T. Zijlstra, J. J. A. Baselmans, S. J. C. Yates, J. R. Gao, and T. M. Klapwijk, Appl. Phys. Lett. **92**, 223502 (2008).
 - [11] A possible contribution to quasiparticle recombination by electron-electron interaction involving a three body process has been proposed in M. Reizer, Phys. Rev. B **61**, 7108 (2000), in which also an exponential increase with decreasing temperature is predicted.
 - [12] P. Verhoeve, R. den Hartog, A. G. Kozorezov, D. Martin, A. van Dordrecht, J. K. Wigmore, and A. Peacock, J. Appl. Phys. **92**, 6072 (2008).
 - [13] T. Nussbaumer, Ph. Lerch, E. Kirk, A. Zehnder, R. Fuchsli, P. F. Meier, and H. R. Ott, Phys. Rev. B **61**, 9719 (2000).
 - [14] L. Li, L. Frunzio, C. M. Wilson, and D. E. Prober, J. Appl. Phys. **93**, 1137 (2003).
 - [15] B. A. Mazin, B. Bumble, P. K. Day, M. E. Eckart, S. Golwala, J. Zmuidzinas, and F. A. Harrison, Appl. Phys. Lett., **89**, 222507 (2006).
 - [16] A. G. Kozorezov, J. K. Wigmore, A. Peacock, A. Poelaert, P. Verhoeve, R. den Hartog, and G. Brammertz, Appl. Phys. Lett. **78**, 3654 (2001).
 - [17] F. Pierre, A. B. Gougam, A. Anthore, H. Pothier, D. Esteve, and N. O. Birge, Phys. Rev. B **68**, 085413 (2003).
 - [18] A. Anthore, F. Pierre, H. Pothier, and D. Esteve, Phys. Rev. Lett. **90**, 076806 (2003).
 - [19] B. Huard, A. Anthore, N. O. Birge, H. Pothier, and D. Esteve, Phys. Rev. Lett. **95**, 036802 (2005).
 - [20] L. Saminadayar, P. Mohanty, R. A. Webb, P. Degiovanni, and C. Bäuerle, Physica E **40**, 12 (2007).
 - [21] A. Yazdani, B. A. Jones, C. P. Lutz, M. F. Crommie, and D. M. Eigler, Science **275**, 1767 (1997).
 - [22] A. Silva and L. B. Ioffe, Phys. Rev. B **71**, 104502 (2005).
 - [23] A. V. Balatsky, I. Vekhter, and J. X. Zhu, Rev. Mod. Phys. **78**, 373 (2006).
 - [24] A. G. Kozorezov, A. A. Golubov, J. K. Wigmore, D. Martin, P. Verhoeve, and R. A. Hijmering, arXiv:0804.1567.